

MCPIP1 restricts HIV infection and is rapidly degraded in activated CD4+ T cells

Shufeng Liu^{a,1}, Chao Qiu^{b,2}, Ruidong Miao^c, Jianhua Zhou^a, Aram Lee^a, Baoming Liu^d, Sandra N. Lester^d, Weihui Fu^b, Lingyan Zhu^b, Linxia Zhang^b, Jianqing Xu^b, Daping Fan^e, Kui Li^d, Mingui Fu^{c,2}, and Tianyi Wang^{a,1,2}

^aDepartment of Infectious Diseases and Microbiology, University of Pittsburgh, Pittsburgh, PA 15261; ^bShanghai Public Health Clinical Center, Institutes of Biomedical Sciences and the Key Laboratory of Medical Molecular Virology of Ministry of Education/Health, Fudan University, Shanghai 201508, China; ^cDepartment of Basic Medical Science, School of Medicine, University of Missouri, Kansas City, MO 64108; ^dDepartments of Microbiology, Immunology, and Biochemistry, University of Tennessee Health Science Center, Memphis, TN 38163; and ^eDepartment of Cell Biology and Anatomy, School of Medicine, University of South Carolina, Columbia, SC 29208

Edited by John M. Coffin, Tufts University School of Medicine, Boston, MA, and approved October 11, 2013 (received for review August 27, 2013)

HIV-1 primarily infects activated CD4+ T cells and macrophages. Quiescent CD4+ T cells, however, possess cellular factors that limit HIV-1 infection at different postentry steps of the viral life cycle. Here, we show that the previously reported immune regulator monocyte chemotactic protein-induced protein 1 (MCPIP1) restricts HIV-1 production in CD4+ T cells. While the ectopic expression of MCPIP1 in cell lines abolished the production of HIV-1, silencing of MCPIP1 enhanced HIV-1 production. Subsequent analysis indicated that MCPIP1 imposes its restriction by decreasing the steady levels of viral mRNA species through its RNase domain. Remarkably, common T-cell stimuli induced the rapid degradation of MCPIP1 in both T-cell lines and quiescent human CD4+ T cells. Lastly, blocking the proteosomal degradation of MCPIP1 by MG132 abrogated HIV-1 production in phorbol 12-myristate 13-acetate/ionomycin-stimulated human CD4+ T cells isolated from healthy donors. Overall, MCPIP1 poses a potent barrier against HIV-1 infection at a posttranscriptional stage. Although the observed HIV restriction conferred by MCPIP1 does not seem to be overcome by any viral protein, it is removed during cellular stimulation. These findings provide insights into the mechanisms of cellular activation-mediated HIV-1 production in CD4+ T cells.

restriction factor | antiviral immunity

Infection by HIV-1 is restricted in cell- and species-specific manners by multiple host factors, such as APOBEC3G, TRIM5 α , Tetherin, and SAM domain and HD domain-containing protein 1 (SAMHD1) (1–9). As the primary targets of HIV-1 in vivo, activated and cycling CD4+ T lymphocytes are more permissive to infection than quiescent CD4+ T cells (10–19). The molecular mechanisms underlying this phenomenon are not fully understood. Ex vivo, CD4+ T cells isolated from periphery blood mononuclear cells (PBMCs) are capable of robustly producing HIV-1 when cultured in the presence of mitogenic stimuli or cytokines, because under such conditions, quiescent CD4+ T cells progress through the cell cycle, proliferate, and thus, stimulate HIV replication and production. An additional possibility is that cell activation may remove unknown blocks to HIV production from CD4+ T cells.

Monocyte chemotactic protein-induced protein 1 (MCPIP1), also known as Zc3h12a or regnase-1, is a critical regulator of the inflammatory response and immune homeostasis (20–24). MCPIP1 belongs to a novel CCCH zinc-finger family of four proteins (MCPIP1–4 or 12A–D), with expression that is highly enriched in immune tissues. Using the KO mouse model, we previously showed that MCPIP1 down-regulates LPS- and cytokine-induced JNK and NF- κ B signaling in macrophages by deubiquitinating TNF receptor-associated factors (21). Matsushita et al. (24, 25) reported that Zc3h12a/MCPIP1 acts as an RNase to promote the mRNA degradation of several inflammatory cytokines.

Here, we show that MCPIP1 potently inhibits HIV-1 infection in human CD4+ T cells. Although MCPIP1 decreases the

steady levels of HIV-1 mRNA species, the inhibition is removed on activation of CD4+ T cells through rapid degradation of MCPIP1.

Results

MCPIP1 Potently Inhibits HIV-1 in Both Transfection and Infection Systems. We first found that coexpression of MCPIP1/Zc3h12a, but not other members from the MCPIP family, with an HIV-1 proviral clone (pNL4.3) in HEK293T inhibited HIV-1 production, which was determined by measuring extracellular p24 levels in the culture supernatant by ELISA and infectious virus production in supernatants determined by TZM-bl assay (Fig. 1 *A* and *B*). CEM-SS, a human T-cell line that is highly permissive to HIV-1 infection, acquired resistance to HIV-1 infection when MCPIP1 was ectopically expressed (Fig. 1*C*). By contrast, the inhibition was not observed in HSV-1 infection (Fig. S1). MCPIP1-mediated HIV-1 inhibition was also observed in both T- and M-tropic prototype viruses (89.6, NL4.3, NL4.3 with Env from AD8, and LAL.2) as well as human T-cell lines (MT2 and MT4), in which the MCPIP1 expression was regulated by doxycycline (Fig. 1 *D* and *E*). Additionally, MCPIP1 inhibited DENV2, encephalomyocarditis virus (EMCV), Yellow fever virus-vaccine strain 17D (YFV-17D), and the human coronavirus OC43 (HCoV-OC43), but it had a marginal effect or no effect on VSV, HSV-1, and new castle diseases virus (NDV) (Figs. S2, S3, S4, S5, and S6). Thus, MCPIP1-mediated restriction seems to be selectively dependent on the virus. To confirm the physiologic relevance of MCPIP1-mediated restriction, endogenous MCPIP1 was knocked down in CEM-SS cells by transfection with siRNA targeting

Significance

Here, we present data showing that monocyte chemotactic protein-induced protein 1 (MCPIP1) acts as an RNase to limit HIV-1 production in resting CD4+ T cells. Unlike those previously identified factors with restrictions that tend to be overcome by virally encoded proteins, MCPIP1 becomes rapidly degraded on activation of human CD4+ T cells. These findings provide insights into the mechanisms of cellular activation-mediated HIV-1 production in CD4+ T cells and represent a breakthrough in the relevant field.

Author contributions: S.L., C.Q., D.F., M.F., and T.W. designed research; S.L., C.Q., R.M., J.Z., A.L., B.L., S.N.L., W.F., L. Zhu, L. Zhang, K.L., and T.W. performed research; J.X. and M.F. contributed new reagents/analytic tools; S.L., C.Q., K.L., M.F., and T.W. analyzed data; and C.Q. and T.W. wrote the paper.

The authors declare no conflict of interest.

This article is a PNAS Direct Submission.

¹Present address: Bioscience Division, SRI International, Harrisonburg, VA 22802.

²To whom correspondence may be addressed. E-mail: qiuchao@fudan.edu.cn, fum@umkc.edu, or tony.wang@sri.com.

This article contains supporting information online at www.pnas.org/lookup/suppl/doi:10.1073/pnas.1316208110/-DCSupplemental.

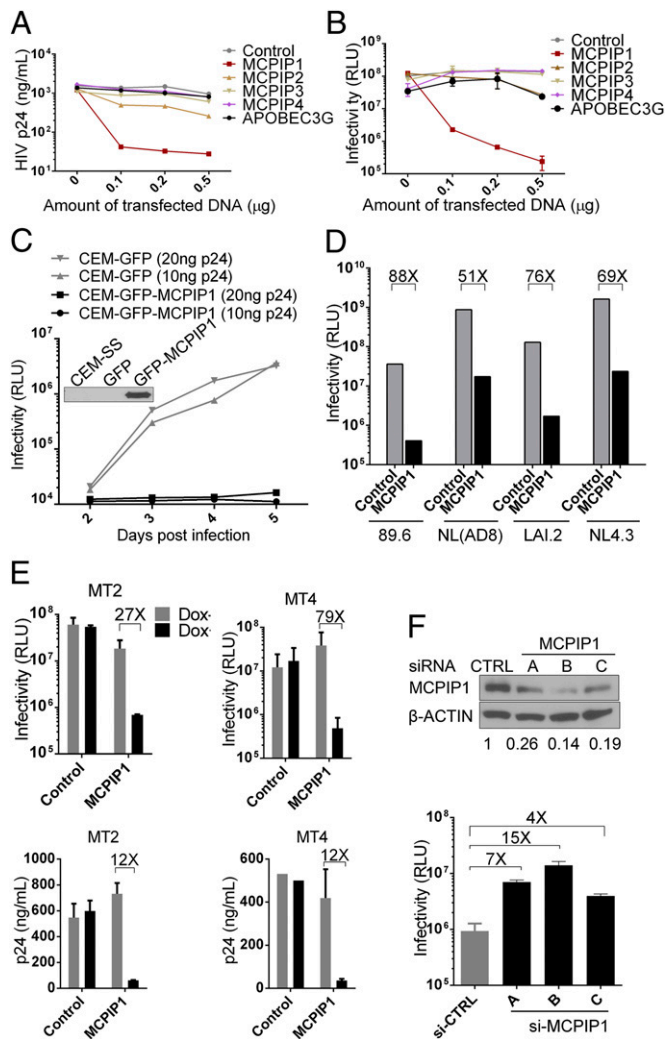


Fig. 1. MCPIP1/ZC3H12A potently inhibits HIV-1 in both transfection and infection systems. (A and B) HIV-1 pNL4.3 proviral construct (0.2 μ g) was cotransfected into 293T cells with 0, 0.1, 0.2, and 0.5 μ g indicated plasmids. At 48 h posttransfection, supernatants were collected for ELISA to determine the secretion of HIV-1 p24 (capsid protein) or TZM-bl assay to measure the production of infectious virus (B). (C) Stable cells derived from CEM-SS (a human T-cell line that is highly permissive to HIV infection) expressing GFP or GFP-MCPIP1 were inoculated with HIV-1 (NL4.3 strain) at two doses (input measured as 10 or 20 ng p24) for 2 h. After extensive wash, cells were further incubated, and supernatants were collected at days 2, 3, 4, and 5 postinfection before TZM-bl assay. (Inset) Western blot image indicates the expression of MCPIP1 in stable cells. (D) Similar assays were performed as in A, except that p89.6 (dual tropic), pNL(AD8) (M tropic), and pLAI.2 (T tropic) proviral DNA were included. A, C, and D are representatives of three independent experiments; B is an average of five independent experiments. A thymidine kinase promoter-driven Renilla luciferase reporter construct was included in all transfection experiments to control for transfection efficiency. (E) MT2 and MT4 human T-cell lines were induced to express GFP-MCPIP1 and then infected by NL4.3 virus. At 48 h postinfection, supernatants were collected for determination of the production of infectious virus and the release of p24. (F) CEM-SS cells were transfected with (Upper) three siRNAs (A, B, and C) by electroporation to knock down the endogenous MCPIP1 (Western blot). The production of infectious HIV-1 from the cells was measured by TZM-bl assays. RLU, relative light unit.

human MCPIP1. As a result of the knockdown, the production of infectious HIV-1 increased (Fig. 1F). A similar observation was made when the knockdown was achieved on exogenously expressed GFP-tagged MCPIP1 in HIV-1 provirus-transfected HEK293 cells (Fig. S7).

MCPIP1 Inhibits HIV-1 at a Posttranscription Step. To identify the stage of the viral life cycle during which MCPIP1 restricts HIV-1, we generated CEM-SS- and HEK293-stable clones that express MCPIP1 in a doxycycline-inducible manner. When doxycycline was added to the cells, the production of infectious virus drastically decreased (Fig. 2A and B). The levels of intracellular viral proteins, including Gag, Env, and Nef, also decreased accordingly (Fig. 2C). However, the copy numbers of provirus DNA did not change in the MCPIP1-expressing cells (Fig. 2D). Additionally, MCPIP1 expression did not suppress the transcriptional activity from the HIV-1 LTR (Fig. 2E), suggesting that MCPIP1 is unlikely to inhibit early steps of HIV life, such as uncoating, reverse transcription, integration, and LTR-driven viral RNA transcription. Rather, MCPIP1 seems to impose its restriction at a late stage after viral RNA transcription. To corroborate this notion, we preinfected CEM-SS with HIV-1 or transfected HEK cells with the proviral construct, pNL4.3, to bypass the steps until integration, and then, we induced the expression of MCPIP1. The production of HIV was nearly abolished after MCPIP1 induction in the HIV preinfected CEM-SS cells and the pNL4.3-transfected HEK cells (Fig. 2F and G). Altogether, these data indicate that MCPIP1 inhibits HIV-1 at a posttranscription step.

RNase Activity of MCPIP1/ZC3H12A Is Required for Its Anti-HIV Activity. Because MCPIP1 possesses RNase activity, we subsequently measured the steady level of unspliced, singly spliced, and multiply spliced HIV-1 RNAs from infected CEM cells by Northern blotting. Fig. 3A shows that there was a significant decrease in all detected HIV-1 RNA species when MCPIP1 was induced in these cells, suggesting that MCPIP1 decreases the abundance of HIV-1 RNA species. In support, knockdown of MCPIP1 by siRNA increased cellular levels of HIV-1 *gag* (unspliced), *vif* (singly spliced), and *tat-ref* (multiply spliced) mRNA (Fig. 3B). Previously, MCPIP1 (20–23, 25) was shown to be an RNase that degrades cytokine mRNAs (24, 25) and cleaves precursor microRNAs (26). Notably, mutations that abolish the RNase activities of MCPIP1 also nullify its anti-HIV activity (Fig. 3C), indicating that MCPIP1 exerts its function through the RNase activity; additionally, the deletion of the zinc-finger domain of MCPIP1 has a similar effect (Fig. 3D), suggesting that the recognition of viral RNA is important. Altogether, these data support the notion that the RNase activity of MCPIP1 degrades HIV-1 RNA species. Similarly, MCPIP1 was recently reported to inhibit Japanese encephalitis virus replication (27). Because MCPIP1 is known to localize to GW bodies, where RNAs are stored and various regulations take place (28), it is possible that MCPIP1 may affect both RNA stability and the translation of viral proteins.

MCPIP1 Is Rapidly Degraded on T-Cell Stimulation. MCPIP1 is highly expressed in tissues, such as thymus, spleen, lung, intestine, and adipose, and was significantly induced by LPS and other stimuli in macrophages (22, 23, 29). Interestingly, although the endogenous level of MCPIP1 is slightly up-regulated in virus-infected A549 or HeLa cells, it remained unchanged in CEM-SS cells infected with HIV-1 (Fig. 4A and Fig. S8). To investigate the potential mechanism by which HIV-1 evades MCPIP1-mediated restriction, we examined the changes in MCPIP1 expression and found that endogenously or exogenously expressed MCPIP1 rapidly disappeared in T-cell lines stimulated with phorbol 12-myristate 13-acetate (PMA)/ionomycin (PMA/Iono) or anti-CD3/anti-CD28 (CME-SS and Jurkat) as well as primary human CD4+ T cells (Fig. 4B and C and Fig. S9). Moreover, culturing primary CD4+ T cells in phytohemagglutinin (PHA) and IL-2 also decreased MCPIP1 at the protein level (Fig. S10). The decrease of MCPIP1 on PMA/Iono stimulation was reversed in the presence of MG132, suggesting that the observed reduction results from proteosomal degradation (Fig. 4D). To explore the relationship between the activation-mediated degradation of MCPIP1 and permissivity to HIV-1 in stimulated CD4+ T cells, we transfected

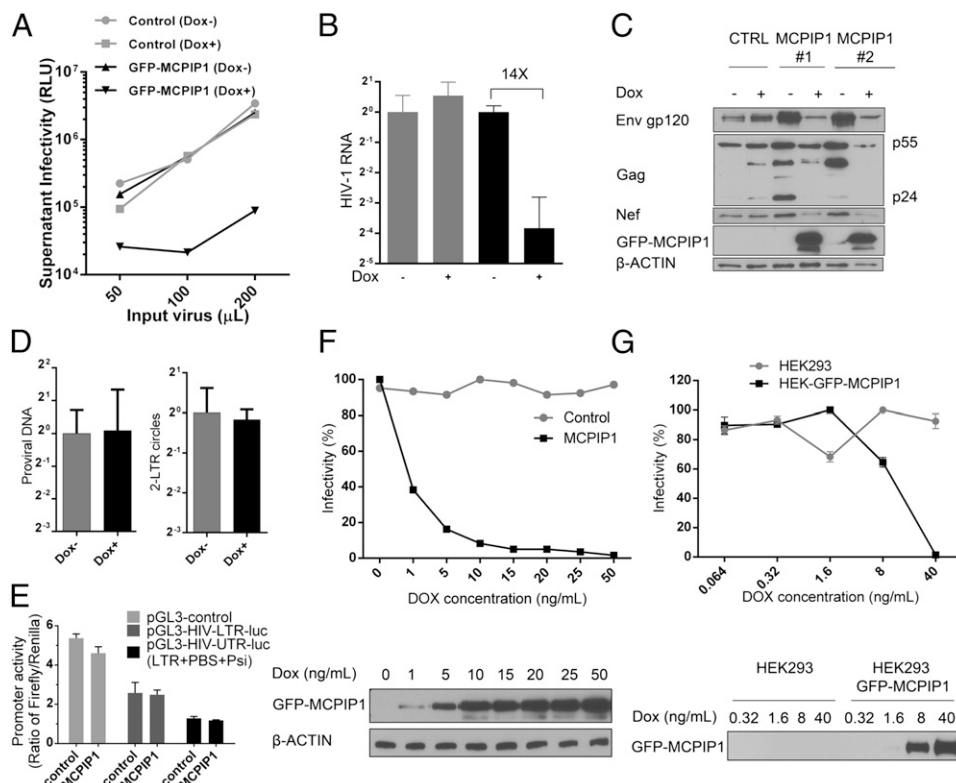


Fig. 2. MCPIP1 inhibits HIV-1 at a posttranscription step. CEM-SS or HEK293T cells were generated to express GFP-tagged MCPIP1 or GFP alone under the control of doxycycline (Dox). (A) CEM-SS cells were incubated with 5 ng/mL Dox overnight to induce GFP-MCPIP1 or GFP and then infected with various amounts of HIV NL4.3; 48 h later, the culture supernatants were analyzed for the infectivity measured by TZM assay. In B, the comparative number of viral RNA was quantified by real-time RT-PCR. An equivalent amount of HCV was added during RNA extraction for normalization. (C) The viral proteins in whole-cell lysates were analyzed by immunoblotting against gp120, gag, nef, and the Dox-induced GFP-tagged MCPIP1. (D) 2-LTR circles were comparatively quantified by real-time PCR. The relative quantification of provirus was performed by Alu-PCR. The level of mtDNA served as a normalization control. (E) The pGL3 reporter containing LTR or UTR (LTR + PBS + Psi) was transiently cotransfected into HEK293T cells with construct expressing MCPIP1 or control vector. The TK promoter-driven vector constitutive expressing Renilla luciferase was used as internal control. The Firefly and Renilla luciferase activities were measured 24 h after transfection. The ratio of Firefly to Renilla is displayed. (F) The CEM-SS cells were inoculated with HIV-1 for 24 h. After being washed, the cells were induced with various amount of Dox to express GFP-tagged MCPIP1 or GFP. At 48 h postinduction, the infectivity of culture supernatant was quantified by TZM assay. The corresponding levels of GFP-tagged MCPIP1 were measured by immunoblotting. (G) The same analysis was done with pNL4.3-transfected 293 cells. HEK293 cells were transiently transfected with pNL4.3. At 24 h posttransfection, cells were induced with various amount of Dox to express GFP-tagged MCPIP1 or GFP. At 48 h postinduction, the infectivity of culture supernatant was quantified by TZM assay. The corresponding level of GFP-tagged MCPIP1 was measured by immunoblotting. RLU, relative light unit.

human CD4⁺ T cells with the pNL4.3 proviral construct and then stimulated the cells with PMA/Iono to allow the release of HIV-1 p24 into supernatants. As expected, the addition of MG132, which prevents the degradation of MCPIP1, ablated the release of HIV p24 from the cells stimulated with PMA/Iono (Fig. 4E).

Discussion

Numerous cellular factors have been implicated in restricting HIV-1 in quiescent CD4⁺ T cells. For example, a primary block has long been noted to limit the reverse transcription of incoming virions (13, 14). The most recently identified deoxynucleoside triphosphate triphosphohydrolase, SAMHD1 (1, 6, 8), seems to be the long-sought cellular factor accounting for this restriction, because SAMHD1 is abundantly expressed in resting CD4⁺ T cells and prevents the reverse transcription of HIV-1 RNA in these cells (18, 30). However, knocking down SAMHD1 in resting CD4⁺ T cells only allowed more effective integration of HIV-1, whereas the production of infectious virus remained impaired (18), implicating additional barriers at later stages of HIV replication. Additionally, although SAMHD1 can be degraded by an HIV-2–encoded protein named Vpx, its expression was shown to be equally abundant in resting and activated CD4⁺ T cells (18). Therefore, it is not difficult to envision that there is

an SAMHD1-independent mechanism that accounts for the observed restriction in resting CD4⁺ T cells and that the restriction is likely to be overcome in activated CD4⁺ T cells. Our findings now shed light on solving the mystery. We previously showed that MCPIP1 deficiency results in a fatal inflammatory phenotype in mice. MCPIP1 KO in mice results in severe T- and B-cell defects (21, 24, 26). Here, we show that, in addition to regulating inflammation, MCPIP1 plays an intriguing role in restricting HIV-1 production in CD4⁺ T cells by decreasing the abundance of HIV RNA species. MCPIP1-mediated HIV-1 inhibition resembles that conferred by zinc-finger antiviral protein in the resistance both factors decrease viral mRNA species (31, 32). MCPIP1 harbors RNase activity, whereas zinc-finger antiviral protein seems to recruit cellular decapping complex to selectively degrade targeted viral mRNA. Whether MCPIP1 directly recognizes and binds viral RNA and thus, degrades viral RNA requires future investigation.

Interestingly, MCPIP1-mediated HIV-1 inhibition is alleviated not by viral factors but by cellular stimulation. A very recent study of regnase-1 (MCPIP1) in KO mice reported that mouse MCPIP1 was rapidly cleaved in activated T cells by a paracaspase termed mucosa-associated lymphoid-tissue lymphoma-translocation gene 1 (MALT1), which has activity that is critically important for activation of T and B lymphocytes (33). Indeed, although the

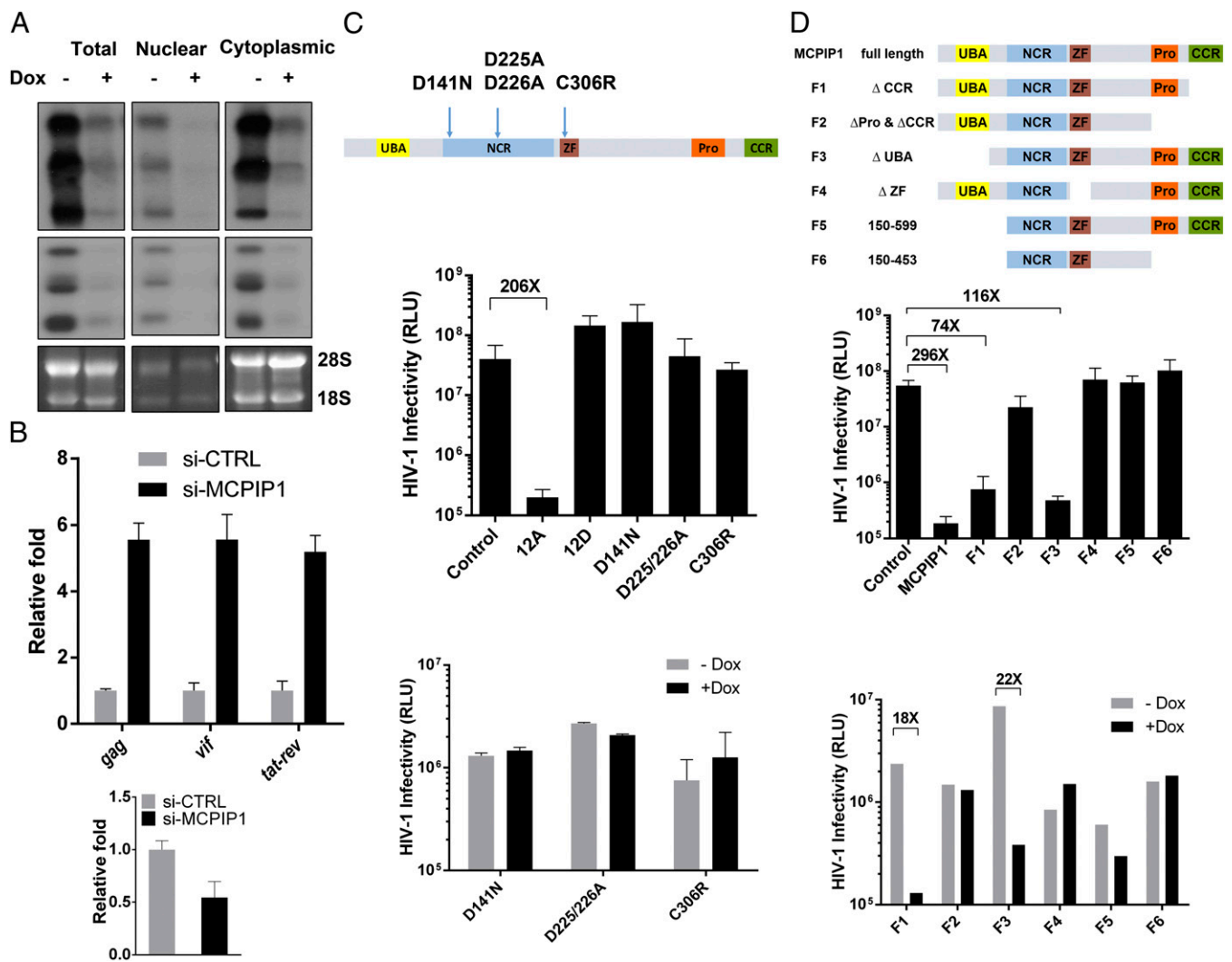


Fig. 3. The RNase activity of MCPIP1 is required for its anti-HIV activity. (A) The viral RNA was extracted from HIV-infected CEM-Dox^{ON}-GFP-MCPIP1 cells [in the presence or absence of doxycycline (Dox)] and subjected to Northern blot analysis for detection of viral RNA species. (Top) Unspliced ~9-kb mRNAs. (Middle) Singly or incompletely spliced ~4-kb mRNAs. (Bottom) Multiply spliced ~1.8-kb mRNAs. The 28S and 18S rRNAs were included as loading controls. (B) CEM-5S cells were electroporated with siRNA against MCPIP1 (construct B) or scrambled siRNA (si-CTRL) at 100 nM. Two days postelectroporation, cells were inoculated with HIV NL4.3. After an additional 2 d of incubation, cellular RNA were isolated and subjected to quantitative RT-PCR analysis. Upper shows the relative fold of change over si-CTRL (HIV Gag, Vif, and Tat-rev mRNA), and Lower shows the knockdown of endogenous MCPIP1. (C, Top) A schematic diagram for point mutations in the putative functional conserved domains of MCPIP1. D141N mutation abolished both deubiquitinating (DUB) and RNase activity; D225/226A lost RNase activity but maintained DUB activity, whereas C306R mutation at the CCCH region lost the DUB activity (21). (Middle) HEK293T cells were transiently cotransfected with pNL4.3 and constructs expressing the indicated mutant form of Flag-tagged MCPIP1; 48 h later, the infectivity of the culture supernatant was measured by TZM assay. (Bottom) CEM-5S cells were also generated to express these mutant forms of MCPIP1 under the control of Dox. After 24 h of incubation with Dox, the cells were infected with HIV; 48 h later, the infectivity of the culture supernatant was measured by TZM assay. (D) The same experiments were done with domain-deleted forms of MCPIP1 (Middle, HEK293 cells; Bottom, CEM-5S cells). $P < 0.005$ ($n = 3$, SD). RLU, relative light unit.

computational analyses have predicted that there are 12 potential PEST regions within human MCPIP1, experimental data suggest that 1 region encompassing residues 96–111 (RQTSPDPCQLP-LVPR) is targeted by MALT1, because mutation of residue 111 from arginine to glycine conferred resistance to MALT1 cleavage (33). It is foreseeable that, after cleavage, MCPIP1 is prone to proteosomal degradation, although this process seems to depend on what type of stimulus is added according to the study. In principle, MCPIP1 may limit HIV-1 infection in CD4⁺ T cells by suppressing the overall cellular activation state through inhibiting NF- κ B activation and the T cell receptor signaling pathway. Our results, however, unequivocally reveal a direct anti-HIV-1 mechanism exerted by MCPIP1 through decreasing the abundance of viral RNA species. Moreover, this antiviral mechanism seems to be shared among fighting several other viruses.

In summary, the loss of MCPIP1 restriction during T-cell activation is likely to contribute to HIV-1 evasion and thus, AIDS pathogenesis. Additional insight into the regulation and consequences of the MCPIP1-imposed restriction in primary CD4⁺ T cells will illuminate pathways for interfering with immunodeficiency in individuals infected with HIV-1.

Materials and Methods

Cells. The human kidney epithelial cell line HEK293 (ATCC CRL-1573), African green monkey kidney epithelial cell lines Vero (ATCC CCL-81) and BSC-1 (ATCC CCL-26), and the baby hamster kidney fibroblast cell line BHK-21 (ATCC CCL-10) were purchased from American Type Culture Collection. Lenti-X 293T was purchased from Clontech. The human T-cell lines CEM-5S, MT-2, MT-4, and Jurkat T, the HIV-1 indicator cell line TZM-bl, and the HeLa cell line were obtained from the National Institutes of Health AIDS Research and Reference

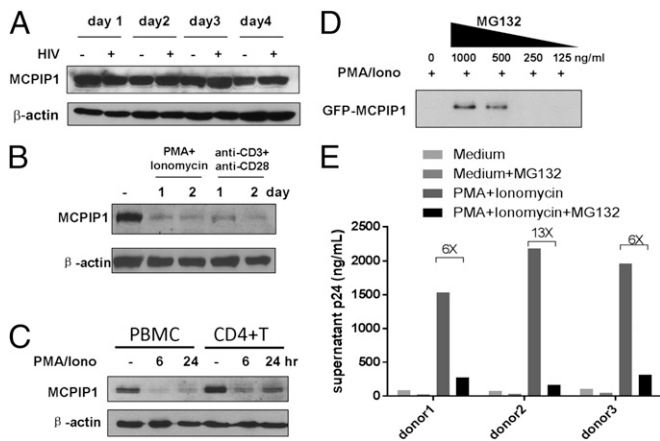


Fig. 4. MCPIP1 is rapidly degraded on T-cell stimulation. (A) CEM-SS cells were infected with HIV for several days. Endogenous MCPIP1 was detected by Western blotting. (B) CEM-SS T cells were treated with PMA/Iono or anti-CD3 and -CD28 antibodies for 1 or 2 d. Endogenous MCPIP1 was detected by Western blotting. (C) Primary human PBMCs and purified CD4+ T cells were stimulated with PMA/Iono for 6 or 24 h. (D) CEM-SS cells expressing GFP-MCPIP1 were cultured in the presence or absence of MG132 for 1 h and then stimulated with PMA/Iono for 18 h. (E) CD4+ T cells from three donors were nucleofected with pNL4.3 and then treated with MG132 for 1 h followed by stimulation of PMA/Iono for 24 h before collection of supernatants. The amount of released p24 was measured by ELISA.

Reagent Program. T-cell lines were cultured in RPMI-1640, whereas TZM-bl, HEK293, BHK-21, and Vero were maintained in DMEM supplemented with 5% (vol/vol) penicillin and streptomycin, 1% nonessential amino acids (NEAA), and 10% (vol/vol) FBS (Gemini Bio-Products). The doxycycline-inducible cell lines were established using the Retro-X Tet-on 3G-inducible expression system (Clontech) following the manufacturer's instructions. The doxycycline-inducible expressions of GFP- or Flag-MCPIP1 were verified in HEK293, HeLa, and CEM-SS cells. The cytotoxicity of overexpression of MCPIP1 was also determined using the CellTiter-Glo Cell Viability Luminescent Assay Kit according to the manufacturer's instructions (Promega) (Fig. S11).

Plasmids. Except where specified otherwise, MCPIP1 expression plasmids, including mutants, have been previously constructed (21). GFP-MCPIP1 was subcloned between Not I/EcoR I sites in the pQCXIP; or the Tet-On construct pRetro-TRE3G.

Antibodies and Reagents. The MCPIP1 rabbit polyclonal antibody was prepared against the human recombinant MCPIP1 protein as described previously (20). Other antibodies used in this study include anti-MCPIP1 (GTX110807; GeneTex), anti-β-actin (4970; Cell Signaling), p24 (ab9071; Abcam), and anti-HCoV-OC43 N (MAB9013; Chemicon). The following reagents were obtained through the National Institutes of Health AIDS Research and Reference Reagent Program: antiserum to HIV-1 gp120 (288; Env) from Michael Phelan and HIV-1 Nef monoclonal antibody (709; Env) from James Hoxie. Rabbit anti-YFV NS3 was a gift from Charles Rice (The Rockefeller University, New York). CD3/CD28 antibodies were purchased from BD Biosciences. Secondary antibodies are purchased from Jackson ImmunoResearch Laboratories, Inc. and Molecular Probes (Invitrogen). PHA, phorbol 12-myristate 13-acetate, and ionomycin were purchased from Sigma.

Viruses. Experiments were performed with NDV-GFP and DENV2 (Thailand 16681 strain) as described (34, 35). EMCV was purchased from American Type Culture Collection (VR-1479). VSV-GFP (provided by S. Sarkar, University of Pittsburgh, Pittsburgh) and HSV1-GFP (gift from Prashant Desai, The Johns Hopkins University, Baltimore) (36) were propagated on Vero cells. YFV-17D (NR-115; BEI Resources) and HCoV-OC43 (ATCC VR-1558) were propagated in Vero E6 and BSC-1 cells, respectively. Viral titers of DENV2 and EMCV were determined on BHK-21 monolayers by plaque assays. Fifty percent tissue culture infectious dose (TCID₅₀) was calculated using the Reed and Muench method. The infectious titers of NDV-GFP, VSV-GFP, and HSV-1 GFP were measured with similar end-point assays by counting GFP-positive cells. The infectivity of YFV-17D- and HCoV-OC43-containing samples was determined

by cytopathic effect-based end-point dilution assay on Vero E6 and BSC-1 cells, respectively, and viral titers were expressed by TCID₅₀/mL.

siRNA Transfection. Three vials of MCPIP1-specific 27mer siRNA duplexes were purchased from OriGene Technologies, Inc. with the following sequences: A, AGCAAGAUGCUCUUAUAAACCCAC (targeting 3'-UTR); B, CCAAAGAUACUGUAGGAUUGGUUCT (targeting 3'-UTR); C, GCCACUCACUUGGAGCACAGGAAG (targeting MCPIP1 coding region); and a universal scrambled negative control siRNA duplex (SR30004). To transfect the 27mer siRNA duplexes into CEM-SS cells, 100 nM duplex was mixed with cells at density of 5 × 10⁶/mL and electroporated using the following settings: 1,230 V, 40 ms, 1 pulse. The transfection efficiency was nearly 100% under such conditions as monitored by transfecting a Cy3-labeled 27mer siRNA from OriGene (SR30002).

Human Primary CD4+ T Lymphocytes. Human PBMCs and purified CD4+ T cells were purchased from HemaCare BioResearch Products and cultured in RPMI-1640 supplemented with 5% (vol/vol) penicillin and streptomycin, 1% NEAA, and 10% (vol/vol) FBS. CD4+ T lymphocytes were cultured at a density of 1 × 10⁶/mL for 3 d in complete RPMI supplemented with 10 μg/mL PHA (Roche). Afterward, cells were washed and further cultured in complete RPMI supplemented with 50 ng/mL human recombinant IL-2 (BD Bioscience) during all experimental processes.

Real-Time PCR. Cells were then washed three times with cold PBS (DPBS) followed by total RNA isolation with TRIzol reagent (Invitrogen). Quantification of RNA was conducted using the QuantiFast SYBR Green RT-PCR Kit (Qiagen) with an in-house developed protocol on a Step One Real-Time PCR System (Applied Biosystems). Primer sequences for the HCV RNA genome were forward: 5'-GCCTAGCCATGGCGTTAGTA-3' and reverse: 5'-CTCCCGGGCCTCGCAAGC-3'. Primer sequences for the housekeeping gene GAPDH were forward: 5'-AGCCGCATCTCTTTTGGTC-3' and reverse: 5'-GAGGGATCTCGTCTCGGAAG-3'.

2-LTR Circles and Integrated Proviruses Assay. Quantitation of HIV cDNA integration by real-time PCR was done by following a published protocol (37). Reaction mixtures contained Taqman gene expression master mix (Life Technologies), 300 nM primers, 100 nM probe, and 500 ng genomic DNA in a 30-μL volume. The PCR conditions were 2 min at 50 °C and 10 min at 95 °C followed by 40 cycles of 15 s at 95 °C and 1 min at 60 °C (1.5 min for Alu PCR).

Quantitation of HIV RNA by Northern Blotting and Quantitative RT-PCR. Experiments were performed using the CEM-SS cell line, in which MCPIP1 expression was controlled by the addition of doxycycline. Compared with the cotransfection system, this inducible system allows analysis of MCPIP1 on HIV RNA degradation in the context of infection but not transfection, which is more problematic for quantitative real-time PCR analysis. Briefly, an NL4.3 virus-infected CEM-SS cell line was left untreated (Dox-) or was treated with doxycycline (Dox+) to induce MCPIP1 expression; 48 h postinfection, nuclear, cytoplasmic, and total RNA were isolated from cells. Northern blotting was performed according to a published protocol (21). Blots were hybridized to a ³²P-labeled probe generated from the 422-nt XhoI/BamHI restriction fragment in the 3'-UTR of pNL4-3, which is present in all HIV-1 mRNAs, following a published protocol (38). On a typical Northern blot, over 40 different HIV-1 primary RNA transcripts, generated by alternative splicing, are detected as three major bands representing three different size classes: unspliced, ~9-kb mRNAs; singly or incompletely spliced, ~4-kb mRNAs; multiply spliced, ~1.8-kb mRNAs (38, 39).

The relative mRNA levels of *gag* (unspliced), *vif* (singly spliced), and *tat-rev* (multiply spliced) were measured by SYBR Green Real-Time PCR in Applied Biosystems StepOne Plus using the following program: (i) 50 °C for 2 min for 1 cycle; (ii) 95 °C for 10 min for 1 cycle; (iii) 95 °C for 15 s, 60 °C for 30 s, and 72 °C for 30 s for 40 cycles; and (iv) 72 °C for 10 min for 1 cycle. The sequences of the primers are shown below.

Name of the primer	Sequence
GAG2 forward	5'-GTGTGAAAATCTCTAGCAGTGG-3'
GAG2 reverse	5'-CGCTCTGCACCCATCTC-3'
Vif forward	5'-GGCGACTGGGACAGC-3'
Vif reverse	5'-CACACAATCATCACCTGCC-3'
Tat-rev forward	5'-ATGGCAGGAAGAAGCGGAG-3'
Tat-rev reverse	5'-ATTCCTTCGGGCTGTGC-3'

HIV-LTR Reporter Gene Assay. Transcription from HIV-1 LTR promoters was measured by a reporter assay, in which the HIV-1 LTR was subcloned in front of the firefly luciferase gene. HEK293T cells in 24-well plates were transfected with 0.2 μ g reporter plasmids and 0.2 μ g pCMV-MAT-Tag-FLAG-MCPIP1 or 0.2 μ g control plasmid together with 0.05 μ g pGL4.74[hRluc/TK] using lipofectamine 2000. The Renilla luciferase reporter, pGL4.74[hRluc/TK], was included to control for transfection efficiency and sample handling. Luciferase activity was measured by the Dual-Luciferase Assay Kit (Promega) using a Veritas Luminometer (Promega).

Immunoblotting. Cells were grown in six-well plates, and lysates were prepared with RIPA buffer [50 mM Tris-HCl, pH 7.4, 1% Nonidet P-40, 0.25% sodium deoxycholate, 150 mM NaCl, 1 mM EDTA, protease inhibitor mixture (Sigma), 1 mM sodium orthovanadate]; insoluble material was precipitated by brief centrifugation. Protein concentration of lysates was determined by BCA Protein Assay (Thermo Scientific). Lysates containing equal amounts of protein were loaded onto 4–20% (vol/vol) Tris-HCl gels (Bio-Rad) and transferred to nitrocellulose membranes. Membranes were blocked in 5%

(vol/vol) nonfat dry milk, probed with the indicated antibodies, and developed with HRP-conjugated secondary antibodies and chemiluminescent substrates (Pierce Biotechnology). Quantification was performed using Gel-Pro Analyzer software.

Statistical Analysis. All experiments were performed at least three times as indicated in the figures. Except where specified, bar graphs were plotted to show mean \pm SD. Statistical analyses were performed using Prism 6. A *P* value < 0.05 in the Student's test was considered statistically significant.

ACKNOWLEDGMENTS. We thank Kelly Huber for technical assistance in running the HIV p24 ELISA. C.Q. is supported by National Natural Science Foundation of China Grant 31000413, the National Grand Program on Key Infectious Disease Control (2012ZX10001), and Chinese Scholarship Council Grant 2011610530. S.N.L. is supported by National Institutes of Health T32 Training Grant AI078906. This work was supported by National Institute of Health Grants AI069285 (to K.L.) and R01DK088787 (to T.W.).

1. Sheehy AM, Gaddis NC, Choi JD, Malim MH (2002) Isolation of a human gene that inhibits HIV-1 infection and is suppressed by the viral Vif protein. *Nature* 418(6898):646–650.
2. Harris RS, et al. (2003) DNA deamination mediates innate immunity to retroviral infection. *Cell* 113(6):803–809.
3. Mangeat B, et al. (2003) Broad antiretroviral defence by human APOBEC3G through lethal editing of nascent reverse transcripts. *Nature* 424(6944):99–103.
4. Zhang H, et al. (2003) The cytidine deaminase CEM15 induces hypermutation in newly synthesized HIV-1 DNA. *Nature* 424(6944):94–98.
5. Berger A, et al. (2011) SAMHD1-deficient CD14+ cells from individuals with Aicardi-Goutières syndrome are highly susceptible to HIV-1 infection. *PLoS Pathog* 7(12):e1002425.
6. Hrecka K, et al. (2011) Vpx relieves inhibition of HIV-1 infection of macrophages mediated by the SAMHD1 protein. *Nature* 474(7353):658–661.
7. Laguette N, et al. (2011) SAMHD1 is the dendritic- and myeloid-cell-specific HIV-1 restriction factor counteracted by Vpx. *Nature* 474(7353):654–657.
8. Goldstone DC, et al. (2011) HIV-1 restriction factor SAMHD1 is a deoxynucleoside triphosphate triphosphohydrolase. *Nature* 480(7377):379–382.
9. Lahouassa H, et al. (2012) SAMHD1 restricts the replication of human immunodeficiency virus type 1 by depleting the intracellular pool of deoxynucleoside triphosphates. *Nat Immunol* 13(3):223–228.
10. Doitsh G, et al. (2010) Abortive HIV infection mediates CD4 T cell depletion and inflammation in human lymphoid tissue. *Cell* 143(5):789–801.
11. Korin YD, Zack JA (1998) Progression to the G1b phase of the cell cycle is required for completion of human immunodeficiency virus type 1 reverse transcription in T cells. *J Virol* 72(4):3161–3168.
12. Pierson TC, et al. (2002) Molecular characterization of preintegration latency in human immunodeficiency virus type 1 infection. *J Virol* 76(17):8518–8531.
13. Stevenson M, Stanwick TL, Dempsey MP, Lamonica CA (1990) HIV-1 replication is controlled at the level of T cell activation and proviral integration. *EMBO J* 9(5):1551–1560.
14. Zack JA, et al. (1990) HIV-1 entry into quiescent primary lymphocytes: Molecular analysis reveals a labile, latent viral structure. *Cell* 61(2):213–222.
15. Dai J, et al. (2009) Human immunodeficiency virus integrates directly into naive resting CD4+ T cells but enters naive cells less efficiently than memory cells. *J Virol* 83(9):4528–4537.
16. Plesa G, et al. (2007) Addition of deoxynucleosides enhances human immunodeficiency virus type 1 integration and 2LTR formation in resting CD4+ T cells. *J Virol* 81(24):13938–13942.
17. Yoder A, et al. (2008) HIV envelope-CXCR4 signaling activates cofilin to overcome cortical actin restriction in resting CD4 T cells. *Cell* 134(5):782–792.
18. Baldauf HM, et al. (2012) SAMHD1 restricts HIV-1 infection in resting CD4(+) T cells. *Nat Med* 18(11):1682–1687.
19. Stevenson M (2003) HIV-1 pathogenesis. *Nat Med* 9(7):853–860.
20. Zhou L, et al. (2006) Monocyte chemoattractant protein-1 induces a novel transcription factor that causes cardiac myocyte apoptosis and ventricular dysfunction. *Circ Res* 98(9):1177–1185.
21. Liang J, et al. (2010) MCP-induced protein 1 deubiquitinates TRAF proteins and negatively regulates JNK and NF-kappaB signaling. *J Exp Med* 207(13):2959–2973.
22. Liang J, Song W, Tromp G, Kolattukudy PE, Fu M (2008) Genome-wide survey and expression profiling of CCH-zinc finger family reveals a functional module in macrophage activation. *PLoS One* 3(8):e2880.
23. Liang J, et al. (2008) A novel CCH-zinc finger protein family regulates proinflammatory activation of macrophages. *J Biol Chem* 283(10):6337–6346.
24. Matsushita K, et al. (2009) Zc3h12a is an RNase essential for controlling immune responses by regulating mRNA decay. *Nature* 458(7242):1185–1190.
25. Iwasaki H, et al. (2011) The I κ B kinase complex regulates the stability of cytokine-encoding mRNA induced by TLR-1L-1R by controlling degradation of regnase-1. *Nat Immunol* 12(12):1167–1175.
26. Suzuki HI, et al. (2011) MCPIP1 ribonuclease antagonizes dicer and terminates microRNA biogenesis through precursor microRNA degradation. *Mol Cell* 44(3):424–436.
27. Lin RJ, et al. (2013) MCPIP1 ribonuclease exhibits broad-spectrum antiviral effects through viral RNA binding and degradation. *Nucleic Acids Res* 41(5):3314–3326.
28. Qi D, et al. (2011) Monocyte chemotactic protein-induced protein 1 (MCPIP1) suppresses stress granule formation and determines apoptosis under stress. *J Biol Chem* 286(48):41692–41700.
29. Qi Y, et al. (2010) MCP-induced protein 1 suppresses TNF α -induced VCAM-1 expression in human endothelial cells. *FEBS Lett* 584(14):3065–3072.
30. Descours B, et al. (2012) SAMHD1 restricts HIV-1 reverse transcription in quiescent CD4(+) T-cells. *Retrovirology* 9:87.
31. Zhu Y, et al. (2011) Zinc-finger antiviral protein inhibits HIV-1 infection by selectively targeting multiply spliced viral mRNAs for degradation. *Proc Natl Acad Sci USA* 108(38):15834–15839.
32. Gao G, Guo X, Goff SP (2002) Inhibition of retroviral RNA production by ZAP, a CCH-type zinc finger protein. *Science* 297(5587):1703–1706.
33. Uehata T, et al. (2013) Malt1-induced cleavage of regnase-1 in CD4(+) helper T cells regulates immune activation. *Cell* 153(5):1036–1049.
34. Biswas N, et al. (2011) The ubiquitin-like protein PLIC-1 or ubiquitin 1 inhibits TRL3-Trif signaling. *PLoS One* 6(6):e21153.
35. McCormick KD, et al. (2012) Development of a robust cytopathic effect-based high-throughput screening assay to identify novel inhibitors of dengue virus. *Antimicrob Agents Chemother* 56(6):3399–3401.
36. Desai P, Person S (1998) Incorporation of the green fluorescent protein into the herpes simplex virus type 1 capsid. *J Virol* 72(9):7563–7568.
37. Ramaswami G, et al. (2012) Accurate identification of human Alu and non-Alu RNA editing sites. *Nat Methods* 9(6):579–581.
38. Exline CM, Feng Z, Stoltzfus CM (2008) Negative and positive mRNA splicing elements act competitively to regulate human immunodeficiency virus type 1 vif gene expression. *J Virol* 82(8):3921–3931.
39. Stoltzfus CM, Madsen JM (2006) Role of viral splicing elements and cellular RNA binding proteins in regulation of HIV-1 alternative RNA splicing. *Curr HIV Res* 4(1):43–55.